ORIGINAL PAPER

Behavioural study of PEMFC during start-up/shutdown cycling for aeronautic applications

Noluntu Dyantyi[1] · Adrian Parsons[1] · Piotr Bujlo[1] · Sivakumar Pasupathi[1]

Abstract

The deployment of proton exchange membrane fuel cell (PEMFC) for aeronautic applications is a value-added energy supply alternative that not only generates useful byproducts (oxygen-depleted air, water and heat) but addresses sensitive issues such as improving health conditions of airport personnel (silent operation minimizes noise) and decreasing greenhouse gas emission (in situ zero emissions). However, the PEMFC is yet to be industrialized due to its fast degrading components. The contribution of the several start-ups and shutdowns (a PEMFC undergoes when operated in aircraft) to the degradation is not well-understood. Hence, this study seeks to explore the effects of start-up/shutdown (SU/SD) cycling on a PEMFC's lifetime. The SU/SD cycling is incorporated with heating to 60 °C and cooling to room temperature to mimic real-life temperature changes encountered in an aircraft. The tested membrane electrode assemblies (MEAs) were characterised for performance and evolution of its components to examine the extent and nature of degradation. More than two-thirds loss of electrochemically active surface area (ECSA) of catalyst, Pt particle growth (4.71–6.41 nm) associated with Ostwald ripening and formation of PtO from adsorption of OH^- by Pt–M surface were identified to be causes of the observed voltage decay at 0.196 mV h^{-1} rate. Hence, it is concluded that SU/SD cycling mostly affects the catalytic component of PEMFC in the aeronautic environment.

Introduction

The PEMFC is a device that operates silently and comprises of solid electrolyte and no moving parts [1, 2]. The PEMFC converts chemical energy from the electrochemical reaction of oxygen and hydrogen into electrical while emitting heat, oxygen-depleted air (ODA) and water as byproducts. These byproducts have useful functions in aircrafts, such as de-icing wing and heating water using emitted heat, fire retardant with the ODA and water generation on board [3]. Furthermore, the PEMFC is an auxiliary power unit (APU) that powers small electrical systems on-board such

as environmental control systems (ECS), in-flight entertainment and recharging batteries [4].

A study by Klebanoff et al. showed that PEMFC could successfully replace the ram air turbine (RAT) emergency backup power system [5]. Hence, leading aircraft manufacturers are working on PEMFC-powered propulsions and APUs as part of establishing "more-electric airplanes" [1, 6]. The "more-electric airplanes" will replace the pneumatically powered and hydraulically powered systems (e.g., ECS and cargo doors) with lighter and more efficient electric systems [7]. Consequently, PEMFC is tested for various aeronautic applications, ranging from nose wheel drive motor, hybrid with batteries, exclusively powering small manned aircrafts to emergency power systems [8–11].

Developments in field and in-flight testing of PEMFC-powered aircrafts includes improving from a hybrid of 20 kW PEMFC with batteries to exclusively 33 kW PEMFC and reaching 1000–2558 m altitude without significant performance loss [8, 12]. The success observed in field testing propelled further testing of PEMFC in laboratory-simulated

✉ Noluntu Dyantyi
3174867@myuwc.ac.za

1 Hydrogen South Africa (HySA) Systems Integration and Technology Validation Competence Centre, South African Institute for Advanced Materials Chemistry, University of the Western Cape, Private Bag X17, Bellville 7535, South Africa

مدينة الملك عبدالعزيز
KACST للعلوم والتقنية

🖄 Springer

aeronautic conditions. The laboratory-simulated aeronautic conditions examined include orientation/inclination and high altitude/low pressure [3, 13–16]. For instance, the effects' inclinations on PEMFC performance were notable when the fuel cells were operated at a low cathode stoichiometry of 1.6 [17]. The notable PEMFC performance losses at high altitude/low pressure (0.7 bar/2200 m altitude) were minimized by increasing the cathode stoichiometry to 1.75 and 2.5 at 1200 m and 2200 m altitude, respectively [16, 18–20]. However, the concerns of increasing cathode stoichiometry to more than 2.5 were membrane drying and power consumption by compressors [19]. The study by Keim et al. and Werner et al. on the quality of the cathode-discharged ODA gas achieved the desired less than 12% ODA oxygen content by operating the fuel cell at 2000 m, 60 °C cell temperature and a high cathode stoichiometry of 3.6 [15, 16, 21]. Again, cathode stoichiometry above 2.5 may damage the stack. Hence, the increase of cathode stoichiometry to 2.5 is taken as an adequate measure to minimize performance losses due to low ambient pressure (0.7 bar at 2200 m) and low oxygen content (16.0% at 2200 m) at high altitudes.

It is safe to say (from the literature survey presented above) that operating and environmental/surrounding conditions have been relatively studied with respect to their effect on PEMFC performance, except for load profile. The typical load profile for aircrafts is as follows: ground taxi, take-off and climb, cruise, descend and landing and ground taxi [4]. Exploring the effects of load profile-related operating conditions on PEMFC performance under aeronautics conditions is essential in enabling the deployment of fuel cells in the aeronautic sector.

Lifetime studies under normal operating conditions are rarely conducted due to time and resource constraints. Hence, fuel cells are tested under conditions that accelerate performance loss and degradation rates using accelerated stress tests (AST) protocols. AST apply different accelerated stressors to determine and predict the durability of fuel cell components by examining known failure mechanisms and major precursors of failure. Each of the AST protocols is designed to focus on a specific fuel cell component. For instance, open circuit voltage (OCV) facilitates chemical attack of the perfluorosulfonic acid (PSFA) membrane by peroxide radicals, whereas relative humidity (RH) cycling causes mechanical degradation of the membrane [5, 22–25]. One of the load profile-related AST that is relevant to aeronautic applications is SU/SD cycling.

Factors that influence fuel cell lifetime under aeronautical conditions are operating temperature, RH and reactants' stoichiometry. In real-world applications, PEMFC is subjected to more than one stressor, either concurrently or simultaneously. De Bruijn's review eloquently demonstrates how a combination of different stressors contributes towards each fuel cell component's degradation [26]. Kim et al. showed

that RH has no significant effect during SU/SD, except at 100% RH [27].

A study by Pei et al. profiled the life expression of a bus driven 43,000 km on a fixed route daily, particularly load-changing cycles, start-up/shutdown cycles, idling cycles and high power conditions [28]. The start–stop cycling, with start-up operating conditions at 60 °C, 1.2/2.5 Sa/Sc, 357 mA cm^{-2}, idling for 1 min at 10 mA cm^{-2}, stop and purge with nitrogen until voltage was zero, caused major degradation. The degradation was attributed to high OCV. Even though there was a follow-up publication by Pei et al. on post-mortem analysis of the membrane electrode assemblies (MEAs), chemical and physical transformations of the fuel cell components caused by the degradation were not examined by common techniques such as SEM, TEM or XRD [29].

SU/SD cycling reported in literature examines the effect of load changes at a fixed temperature, which is not necessarily representative of the actual start-up or shutdown, as heating and cooling occur concurrently. Hence, the aim of this study is to evaluate the behaviour of PEMFC operated at 60 °C and exposed to SU/SD with heating and cooling as it would happen during aircraft operation. The PEMFC was characterised for the extent and nature of degradation to better understand its behaviour in the aeronautic environment.

Materials and methods

Setup

The low-temperature PEMFC single cell (see Fig. 1) used for testing consisted of a 25 cm^2 commercial MEA, assembled in a commercial single cell fixture made of graphite bipolar plates with a serpentine/parallel flow pattern design and gold-plated current collectors. Both anode and cathode catalyst loadings were 1.0 mg cm^{-2} Pt.

The single cell was tested using the Greenlight G20 Fuel Cell Test Station. The fuel cell was operated at atmospheric pressure with pure hydrogen and air supplied to the anode and cathode, respectively. The stoichiometry used was 1.8/2.5 for the anode and cathode. The MEA was activated by applying a constant voltage of 0.7 V to a cell operating at 60 °C, supplied with fully humidified (100% RH) reactants, at anode/cathode stoichiometry of 1.8/2 for 100 h. Fuel cell parameters such as operating temperature, dew point, stoichiometry/flow rates and load were controlled using Greenlight's Emerald™ control and automation software.

Test conditions

The MEA was subjected to SU/SD cycling with heating and cooling to mimic aeronautic conditions as shown in

Fig. 1 Components of the single cell used in this study and schematic illustration of reactants' flow and chemical reactions taking place
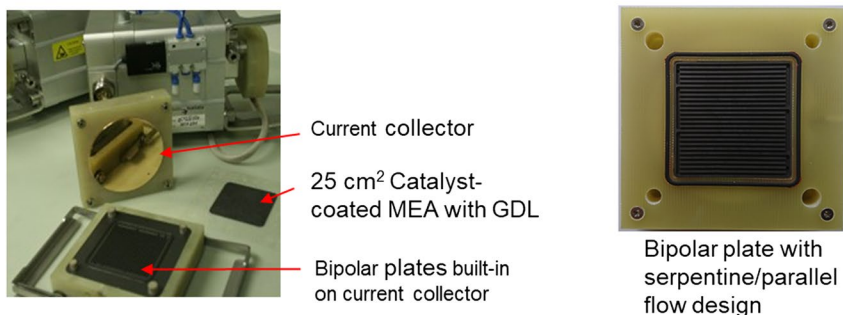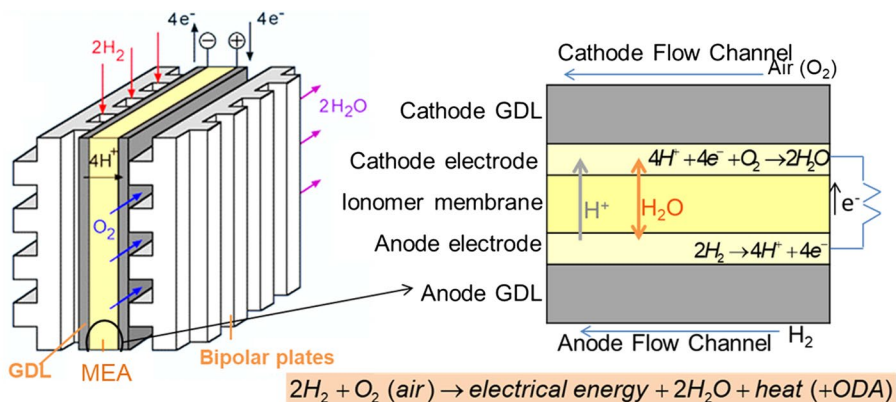

Fig. 2 Schematic diagram of SU/SD cycle (heating up to 60 °C and cooling down to room temperature) used during experimental part of the work. A voltage of 0.7 V was imposed during the heating and cooling. Voltage was measured at the imposed current when measuring IV curve and purging
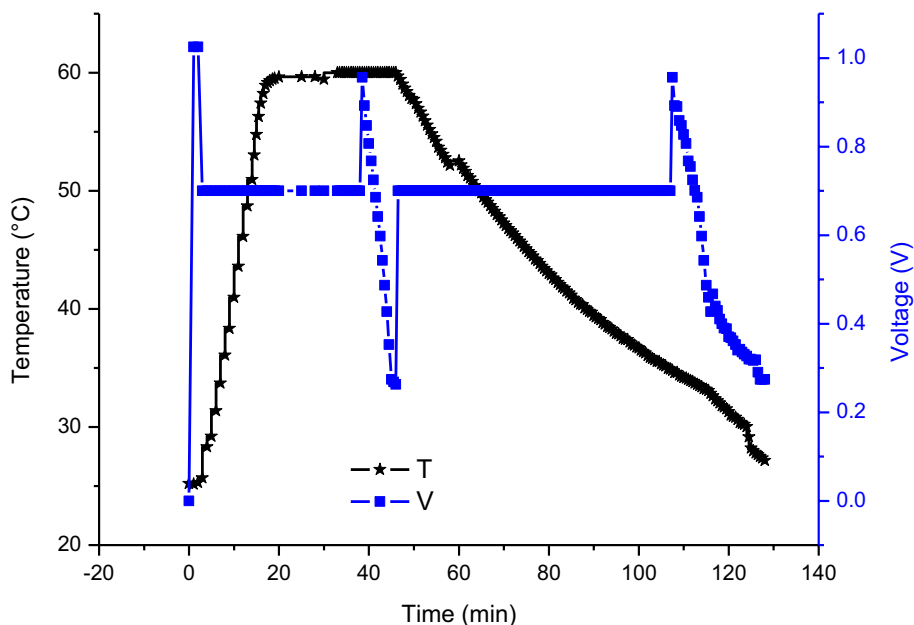

Fig. 2. The single cell was heated to 60 °C at 0.7 V, 100% RH and 1.8/2.5 anode/cathode stoichiometric ratio. When the fuel cell reached 60 °C and stabilized for 15 min, a polarization (IV) curve was taken and the cell was cooled to room temperature, followed by 5 min rest prior to restart. The cell was purged with nitrogen for only 5 min at the end of each cycle to minimize hydrogen/air interface until voltage reaches zero since purging is impractical in real operation of aircraft fuel cells.

Electrochemical analysis

An IV curve provides information on overall fuel cell performance and is used to estimate the overall degradation

rate using voltage decay over test duration. The IV curves were measured using the Emerald™ software test station in galvanostatic mode from 0.0 to 0.7 mA cm^{-2}. Operating conditions were kept similar to the SU/SD cycling with 60 °C cell temperature, 65 °C dew point temperature and 1.8/2.5 stoichiometric ratio. The results obtained were used to compute the average degradation rate (ADR) by calculating the difference between initial and final voltage over the test duration using Eq. 1:

$$ADR = \frac{\text{Initial voltage} - \text{Final voltage}}{\text{Test duration}}. \qquad (1)$$

The fresh and tested MEAs were characterised for electrochemical properties using cyclic voltammetry (CV). The CV measurements were taken using the Autolab PGSTAT302N potentiostat with FRA2 module controlled by Nova software. The CV was measured at 30 °C, a voltage range of 0.015–1.00 V and a sweep rate of 30 mV s^{-1}. The gas supply for the CV was hydrogen and nitrogen at anode and cathode, respectively.

Chemical/physical analysis

Small pieces were cut out from the MEAs and characterised using high-resolution scanning electron microscopy coupled with energy-dispersive spectroscopy (HR-SEM/EDS) and X-ray diffraction (XRD). ZEISS MERLIN HR-SEM/EDS was used to characterise cross-sections of the MEAs for chemical composition and particle migration/redeposition. Bruker D8 high-resolution X-ray diffractometer with Vantec detector was used to analyse the crystal structure, phase purity and particle size distribution (PSD). Electrode powder samples were also examined for changes in the structure of the catalyst layer by capturing Pt transformation due to particle migration, particle growth from agglomeration and changes in the structure of the membrane surface. This was done through the use of high-resolution transmission electron microscopy (HR-TEM) and HR-SEM/EDS. The HR-TEM used was Hitachi H800 200 kV instrument fitted with a digital image acquisition system.

Results and discussions

Overall performance

PEMFC performance is a measure of the ability of fuel cells to generate the required power output. Overall degradation, however, is quantified as the rate of voltage decay. The fuel cell was subjected to 600 SU/SD cycles that took 120 min each and the voltage measured at 400 mA cm^{-2} decreased from 0.3359–0.1003 V, with a degradation rate of 0.196 mV h^{-1}. Figure 3 shows the recorded changes in voltage
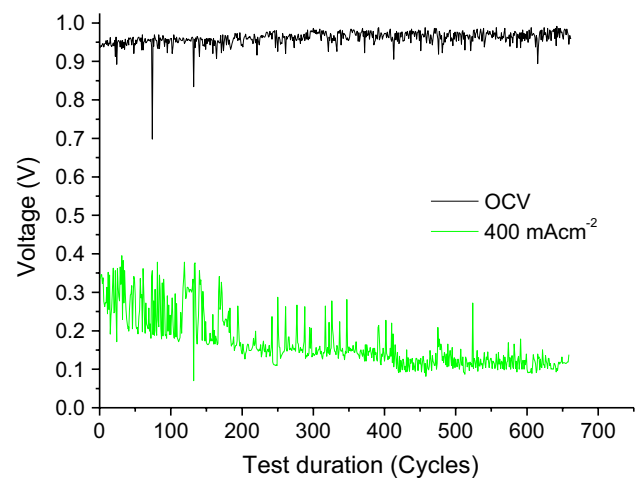
Fig. 3 Voltage evolution at OCV and 400 mA cm^{-2} during SU/SD cycling carried out between room temperature and 60 °C for 600 cycles at 100% RH, atmospheric pressure and stoichiometric ratio of 1.8/2.5 anode/cathode
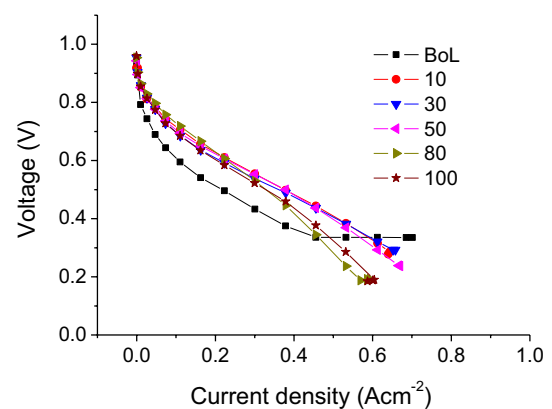

Fig. 4 The IV curves taken within the first 100 SU/SD cycles at random intervals. The IV curves were measured at 60 °C, 100% RH, atmospheric pressure and stoichiometric ratio of 1.8/2.5 anode/cathode

at OCV and 400 mA cm^{-2}. 400 mA cm^{-2} (equivalent to 10 A) was chosen as the current density representative of the ohmic loss region according to polarization curve diagram. Voltage decay was more apparent at higher current density relative to when there was no current drawn. Similarly to Kim et al. and Jo et al., voltage loss at the OCV region was minute [27, 30]. The insignificant voltage decay at the activation region suggests minor changes in kinetics of oxygen reduction reaction (ORR), implying that there are no perforations in the membrane [31].

The IV curve of a pristine MEA recorded prior to the test is regarded as beginning of life (BoL). Figure 4 demonstrates a performance improvement observed during the first 100 cycles. The peak in current at the beginning of the tests may
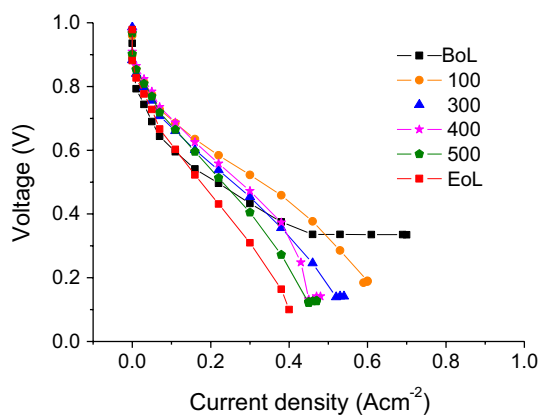
Fig. 5 The IV curves of the fuel cell prior to and after the SU/SD cycling test at 60 °C, 100% RH and 1.8/2.5 anode/cathode stoichiometry

be due to continued MEA activation. On the other hand, a significant performance drop was observed immediately after 100 cycles at high current densities and voltage continued to drop until the end of the test (EoL), 600 cycles as shown in Fig. 5.

The sudden decrease observed after 100 cycles at high current densities may be caused by mass transport limitations, since PEMFC requires a higher active surface area to meet the demand of the chemical reactions compared to low current densities [32]. Kim et al. also reported that full humidification may lead to excess water that blocks the electrode surface area and subsequently results in temporary reactants' starvation [27]. The review by Yu et al. highlighted that SU/SD degradation is minimal at low temperatures and humidity [33]. Given that the rate of water generation is much faster at high current density compared to low current density, the IV curves results attest that higher humidity introduces additional water into the cell that causes flooding and subsequently promotes degradation. Full humidification was chosen as a worse-case scenario in this study, since PEMFCs operating in aeronautic conditions are likely to be periodically flooded due to varying load demands.

Electrochemical evolution

The CV was employed as a complimentary in situ electrochemical technique to the IV curve, since it provides information on the catalyst activity. Linse et al. discovered that voltage loss after SU/SD cycling was due to mass transport limitations and the formation of isolated electrode areas/Pt agglomeration [34]. The latter reflects electrode degradation, which is associated with high voltage and starvation caused by flooding. As a result, the fuel cell was characterised for catalyst activity using CV. Expectedly so, the

voltammograms in Fig. 6 show a significant loss of catalyst activity after 600 cycles, taken as end of life (EoL).

The CV data was further processed to estimate ECSA through Eq. 2. The ECSA was 58.88 and 22.56 cm g^2 Pt(gPt)$^{-1}$ at beginning and end of tests, respectively. The calculation showed that more than two-thirds of catalyst activity was lost:

$$\text{ECSA} = \frac{Q}{210 \times 10^{-3} \times \text{Pt loading}}, \tag{2}$$

where Q represents the charge (mC cm^{-2}) associated with the hydrogen adsorption/desorption, Pt loading is the loading of platinum at the studied electrode (gPt cm^{-2} Pt), 210×10^{-3} is the hydrogen adsorption/desorption charge (mC cm^{-2} Pt) on a smooth Pt electrode.

Exploration of degradation mechanisms

To examine the cause of fuel cell performance and ECSA losses, changes in PSD of cathode Pt/C catalysts were analysed through HR-TEM and XRD. The micrographs and diffractograms were taken before and after SU/SD cycling, as shown in Figs. 7 and 8, respectively.

The PSD shown in Fig. 9 was estimated by calculating the average particle diameter using ImageJ software and qualitatively through observing peak properties of the diffractograms. ImageJ software takes into account the known scale, resolution and magnification in which HR-TEM images were measured.

High voltages favour platinum dissolution and Wang et al. observed a higher concentration of Pt at 0.9 V [36]. On the other hand, Pt particles are easily redeposited at reverse current conditions created by the SU/SD [30]. Due to high equilibrium potential of dissolution, Pt ions tend to redeposit
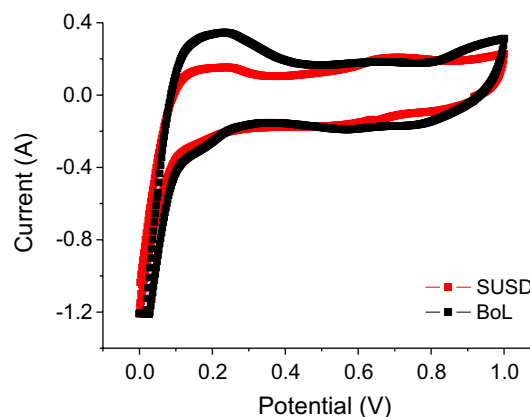

Fig. 6 Cyclic voltammetry of a fresh (BoL) and tested MEA (SUSD) measured at 30 °C, 100% RH and a voltage range of 0.015–1.00 V and a sweep rate of 30 mVs^{-1}. The anode and cathode were supplied with hydrogen and nitrogen gases

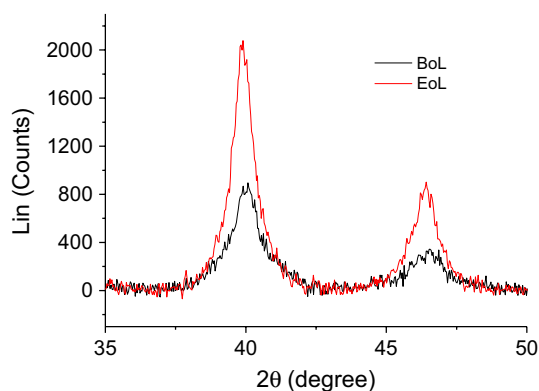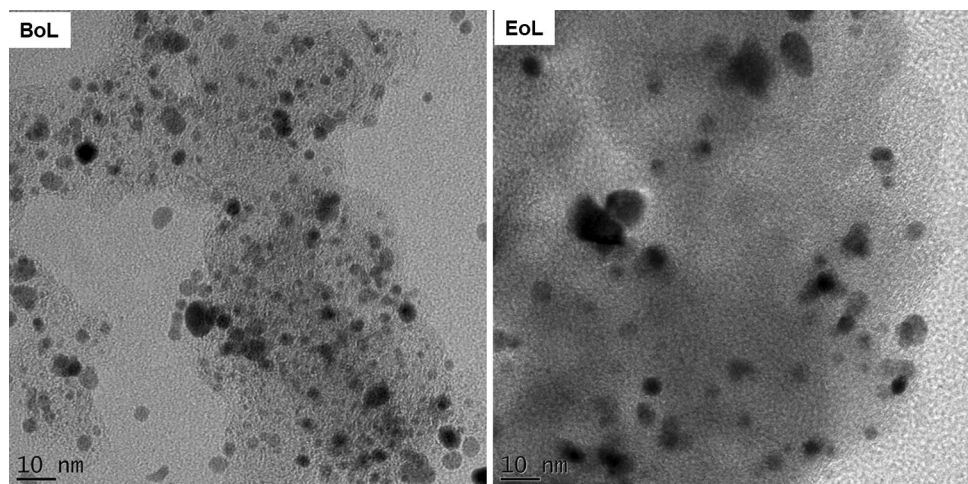**Fig. 7** HR-TEM micrographs of fresh (BoL) and tested (EoL) cathode catalysts

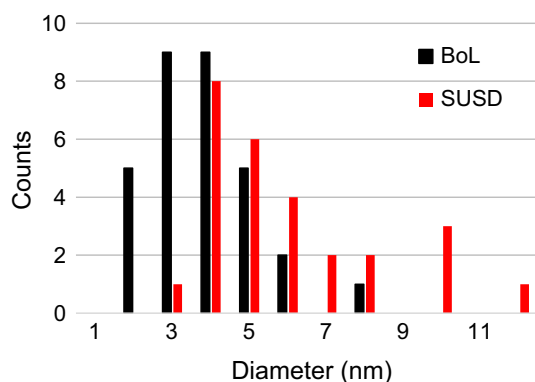**Fig. 8** XRD patterns of cathode before (BoL) and after SU/SD cycling (EoL)

Fig. 9 Relative particle size distribution of Pt particles at beginning of life (BoL) and after SU/SD cycling (EoL)

onto larger Pt particles in the cathode and thus undergo Ostwald ripening to minimize surface energy [37]. Hence, the increased average particle size from 4.71 to 6.41 nm (Fig. 9) and HR-TEM micrographs (Fig. 7) suggest that the particles experienced Ostwald ripening, migration/dissolution and

redeposition. Zhao et al. noted that narrower XRD peaks indicate larger Pt particles [35]. The particle growth corresponds to the loss of ECSA (Fig. 6) and narrower XRD peaks (Fig. 8). Therefore, Pt particle agglomeration may be attributed to a loss of ECSA and be one of the causes of voltage decay.

An additional reason for ECSA loss may be the adsorption of OH^- on Pt–M surfaces which forms PtO. Pt sintering mostly occurs at cathode due to chemical oxidation of Pt into PtO by residual oxygen present in the cathode layer, following the mechanism in Eqs. 3 and 4 [38]. The hydrogen and oxygen presence may be due to the short time of purging, since IV curves data hinted no signs of crossover:

$$Pt^{2+} + H_2 \; \rightarrow \; Pt + 2H^+, \tag{3}$$

$$Pt + {}^1\!/_2 O_2 \; \rightarrow \; PtO. \tag{4}$$

Loose Pt particles, due to a collapse of support, move freely and redeposit either on other Pt particles or on the membrane. The latter was neither notable nor studied further due to unnoticeable membrane degradation and being limited by the scope of this research. The former has been shown by the different analytical techniques used in this study, such as HR-TEM and XRD to be demonstrating Pt particle growth.

The observed delamination on cross-section in Fig. 9 supports the hypothesis of loose Pt particles due to carbon corrosion. Turquoise Pt and purple S particles in Fig. 10 are visible on all the layers captured by HRSM/EDS at EoL, implying migration and redeposition.

Therefore, the loss of ECSA may be partly attributed to carbon support corrosion.

Table 1 contains elemental compositions of the pristine and tested MEAs as acquired from HR-SEM/EDS. The presence of oxygen on the tested MEA substantiates the occurrence of the reactions outlined in Eqs. 3 and 4 above. The

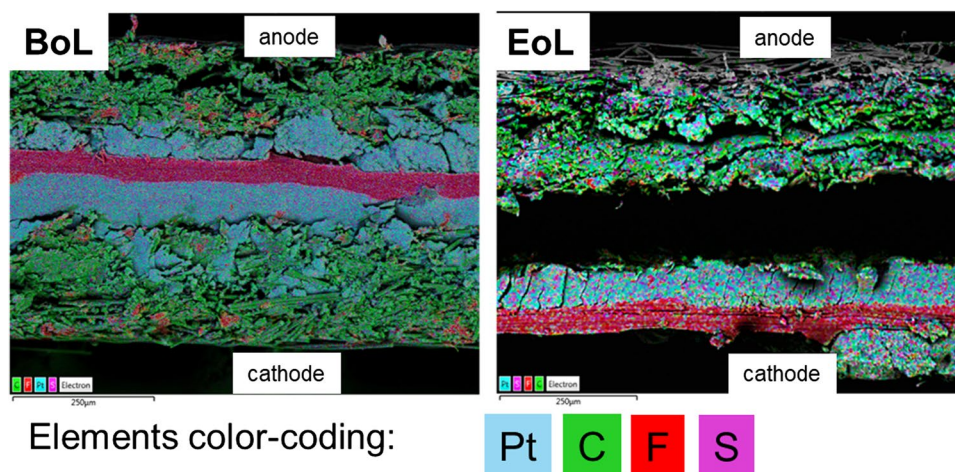**Fig. 10** HR-SEM/EDS layered image of MEA's cross-section before (BoL) and after (EoL) SU/SD cycling

Table 1 Elemental composition of a pristine and tested MEA as obtained from HR-SEM/EDS

Test/element	BoL (wt%)	EoL (wt%)
Carbon	70.07	59.42
Fluoride	2.96	7.95
Sulphur	0.72	0.66
Platinum	26.26	27.21
Oxygen	–	4.76

minute change in concentrations proves that Pt did not leach out but rather migrated and redeposited.

Carbon leached out after 600 cycles (EoL), which indicates corrosion of the catalyst support. Carbon support corrosion is prevalent at high voltage [28, 39]. Flooding, as likely to occur at high current densities for a fully humidified cell exposed to variable load demands, is reportedly blocking catalyst reactive sites and promotes carbon corrosion [40, 41]. Pt agglomeration tends to be aggravated by carbon corrosion. Therefore, the loss of ECSA may be partly attributed to carbon support corrosion.

Conclusion

The aim of this study was to examine the effect of SU/SD cycling on the performance of PEMFC operating in an aeronautic environment. The aeronautic environment was simulated by incorporating heating to 60 °C and cooling to room temperature while operating at 1.8:2.5 anode/cathode stoichiometric ratio. This specific stoichiometric ratio was selected, because increasing cathode to 2.5 minimizes performance loss associated with high altitudes and improves quality of ODA for multifunctional fuel cells.

The ultimate objective of this research was to collect and document AST data relevant to aeronautic applications. In doing so, understanding of PEMFC behaviour in an aeronautic environment will be enhanced and thus its performance and state of health can be better managed.

The studied MEA was characterised for overall performance and ECSA using the IV curve and the CV. Physical and chemical properties such as elemental composition and particle size distribution were evaluated using HR-SEM/EDS, XRD and HR-TEM.

Voltage evolution recorded during the test showed average degradation of 0.196 mV h^{-1}. The loss of ECSA revealed that the observed performance loss may be attributed to catalyst degradation. Furthermore, Pt particle agglomeration (shown by increased average particle size) suggests that Pt redeposition is one of the causes of loss of ECSA, which is evidence for catalyst degradation. The presence of oxygen from the HR-SEM/EDS results proves oxidation of Pt into PtO which covers the catalyst surface area and hinders the chemical reactions from taking place. Thus, it can be concluded that SU/SD-induced degradation on PEMFC operated in aeronautic conditions is caused by catalyst degradation in the form of Pt particle agglomeration due to redeposition and oxidation of Pt into PtO.

References

1. Seidel Jonathan, A., Sehra Arun, K., Colantonio Renato, O.: NASA aeropropulsion research: Looking forward. NASA, Glenn Research Center, Cleveland (2001)
2. Friedrich, K.A., et al.: Fuel cell systems for aircraft application. ECS Trans. **25**, 193–202 (2009)
3. Renouard-Vallet, G., et al.: Fuel cells for civil aircraft application: on-board production of power, water and inert gas. Chem. Eng. Res. Design **90**, 3–10 (2012)
4. Pratt, J.W., et al.: Proton exchange membrane fuel cells for electrical power generation on-board commercial airplanes. Appl. Energy **101**, 776–796 (2013)
5. Klebanoff, L.E., Cornelius, C.J.: Analysis of hydrogen storage for a fuel cell emergency power system (FCEPS) for commercial aircraft. In: Annual Merit Review and Peer Evaluation Meeting, 9–13 May, Arlington, Virginia (2011)
6. Daggett, D. L., Eelman, S. and Kristiansson, G.: Fuel cell APU for commercial aircraft. In: AIAA/ICAS International air and space symposium and exposition: the next 100 years, 14–17 July, Dayton, Ohio, pp. 1–9 (2003)
7. Eelman, S., del Pozo y de Poza, I., Krieg, T.: Fuel cell APU's in commercial aircraft—an assessment of SOFC and PEMFC concepts. In: 24th International congress of the aeronautical sciences, 29 Aug–3 Sept, Yokohama, Japan, pp. 1–10 (2004)
8. Lapeña-Rey, N., et al.: Environmentally friendly power sources for aerospace applications. J. Power Sources **181**, 353–362 (2008)
9. Romeo, G.: The First European Commision Funded aircraft powered by a hydrogen fuel cell took its first flight. https://fuelcellsworks.com/archives/2010/06/15/first-european-commission-funded-aircraft-powered-by-a-hydrogen-fuel-cell-takes-first-flight/ (2010). Accessed 23 July 2015
10. DLR International Press Release: DLR Airbus A320 ATRA taxis uses fuel cell-powered nose wheel for the first time. Available from: http://www.dlr.de/dlr/presse/en/desktopdefault.aspx/tabid-10307/470_read-931/year-2011/#/gallery/2079 (2011). Accessed 11 June 2015
11. Boeing International Press Release.: 787 electrical system. Available from: http://787updates.newairplane.com/787-Electrical-Systems/787-Electrical-System (2013). Accessed 11 June 2015
12. Rathke, P., et al.: Long distance flight testing with fuel cell powered aircraft antares DLR-H2. https://www.dglr.de/publikationen/2014/301219.pdf (2013). Accessed 11 June 2015
13. Rouss, V., et al.: Mechanical behaviour of a fuel cell stack under vibrating conditions linked to aircraft applications part I: experimental. Int. J. Hydrogen Energy **33**, 6755–6765 (2008)
14. Bégot, S., et al.: Fuel cell climatic tests designed for new configured aircraft application. Energy Convers. Manage. **51**, 1522–1535 (2010)
15. Keim, M., et al.: Multifunctional fuel cell system in an aircraft environment: an investigation focusing on fuel tank inerting and water generation. Aerosp. Sci. Technol. **29**, 330–338 (2013)
16. Werner, C., et al.: Characteristics of PEMFC operation in ambient- and low-pressure environment considering the fuel cell humidification. CEAS Aeronaut. J. **6**, 1–15 (2014)
17. Renouard-Vallet, G., et al.: Improving the environmental impact of civil aircraft by fuel cell technology: concepts and technological progress. Energy Environ. Sci. **3**, 1458–1468 (2010)
18. Uno, M., et al.: Development and demonstration flight of a fuel cell system for high-altitude balloons. J. Power Sources **193**, 788–796 (2009)
19. Hordé, T., Achard, P., Metkemeijer, R.: PEMFC application for aviation: experimental and numerical study of sensitivity to altitude. Int. J. Hydrogen Energy **37**, 10818–10829 (2012)
20. Kallo, J., et al.: Fuel cell system development and testing for aircraft applications, in 18th World Hydrogen Energy Conference, 16–21 May, pp. 435–444. Essen, Germany (2010)
21. Werner, C., Busemeyer, L., Kallo, J.: The impact of operating parameters and system architecture on the water management of a multifunctional PEMFC system. Int. J. Hydrogen Energy **40**, 11595–11603 (2015)
22. Inaba, M., et al.: Gas crossover and membrane degradation in polymer electrolyte fuel cells. Electrochim. Acta **51**, 5746–5753 (2006)
23. Makharia, R., et al.: Durable PEM fuel cell electrode materials: requirements and benchmarking methodologies. ECS Trans. **1**, 3–18 (2006)
24. Tang, H., et al.: A degradation study of Nafion proton exchange membrane of PEM fuel cells. J. Power Sources **170**, 85–92 (2007)
25. Zhang, S., et al.: Effects of open-circuit operation on membrane and catalyst layer degradation in proton exchange membrane fuel cells. J. Power Sources **195**, 1142–1148 (2010). https://doi.org/10.1016/j.jpowsour.2009.08.070
26. de Bruijn, F.A., Dam, V.A.T., Janssen, G.J.M.: Review: durability and degradation issues of PEM fuel cell components. Fuel Cells **8**, 3–22 (2008)
27. Kim, J.H., et al.: Effects of cathode inlet relative humidity on PEMFC durability during startup-shutdown cycling. J. Electrochem. Soc. **157**, B104–B112 (2010)
28. Pei, P., Chang, Q., Tang, T.: A quick evaluating method for automotive fuel cell lifetime. Int. J. Hydrogen Energy **33**, 3829–3836 (2008)
29. Pei, P., et al.: Analysis on the PEM fuel cells after accelerated life experiment. Int. J. Hydrogen Energy **35**, 3147–3151 (2010)
30. Jo, Y.Y., et al.: Degradation of polymer electrolyte membrane fuel cells repetitively exposed to reverse current condition under different temperature. J. Power Sources **196**, 9906–9915 (2011). https://doi.org/10.1016/j.jpowsour.2011.08.035
31. Shan, J., et al.: Local resolved investigation of PEMFC performance degradation mechanism during dynamic driving cycle. Int. J. Hydrogen Energy **41**, 4239–4250 (2016)
32. Lin, R., et al.: Investigating the effect of start-up and shut-down cycles on the performance of the proton exchange membrane fuel cell by segmented cell technology. Int. J. Hydrogen Energy **40**, 14952–14962 (2015). https://doi.org/10.1016/j.ijhydene.2015.09.042
33. Yu, Y., et al.: A review on performance degradation of proton exchange membrane fuel cells during startup and shutdown processes: causes, consequences, and mitigation strategies. J. Power Sources **205**, 10–23 (2012)
34. Linse, N.: Start/stop phenomena in polymer electrolyte fuel cells, pp. 1–221, PhD Thesis (2012)
35. Zhao, M., et al.: Influence of membrane thickness on membrane degradation and platinum agglomeration under long-term open circuit voltage conditions. Electrochim. Acta **153**, 254–262 (2015). https://doi.org/10.1016/j.electacta.2014.12.024
36. Wang, X., Kumar, R., Myers, D.: Effect of voltage on platinum dissolution relevance to polymer electrolyte fuel cells. Electrochem. Solid-State Lett. **9**, A225–A227 (2006)
37. Ferreira, P.J., et al.: Instability of Pt/C electrocatalysts in proton exchange membrane fuel cells. A mechanistic fuel cells. J. Electrochem. Soc. **152**, A2256–A2271 (2005)
38. Chung, C.G., et al.: Degradation mechanism of electrocatalyst during long-term operation of PEMFC. Int. J. Hydrogen Energy **34**, 8974–8981 (2009)
39. Zhang, Y., et al.: Study of the degradation mechanisms of carbon-supported platinum fuel cells catalyst via different accelerated stress test. J. Power Sources **273**, 62–69 (2015)
40. Maass, S., et al.: Carbon support oxidation in PEM fuel cell cathodes. J. Power Sources **176**, 444–451 (2008)
41. Liu, M., et al.: Diagnosis of membrane electrode assembly degradation with drive cycle test technique. Int. J. Hydrogen Energy **39**, 14370–14375 (2014)